

Biotransformation of 3-Amino-5,6,7,8-tetrahydro-2-[4-[4-(quinolin-2-yl)piperazin-1-yl]butyl]quinazolin-4(3H)-one (TZB-30878), a Novel 5-Hydroxytryptamine (5-HT)_{1A} Agonist/5-HT₃ Antagonist, in Human Hepatic Cytochrome P450 Enzymes

Kouichi Minato, Ryota Suzuki, Akira Asagarasu, Teruaki Matsui, and Michitaka Sato

Pharmacokinetics Research Department (K.M., R.S.) and Synthetic Research Department (A.A., T.M., M.S.), ASKA Pharmaceutical Co., Ltd., Kawasaki, Japan

Received August 13, 2007; accepted January 28, 2008

ABSTRACT:

3-Amino-5,6,7,8-tetrahydro-2-[4-[4-(quinolin-2-yl)piperazin-1-yl]butyl]quinazolin-4(3H)-one (TZB-30878), a novel 5-hydroxytryptamine (5-HT)_{1A} agonist/5-HT₃ antagonist, is currently under development for the treatment of irritable bowel syndrome. The objective of this investigation was to obtain information on the biotransformation of TZB-30878. This compound has quinazoline, piperazine, and quinoline rings. Metabolites of [quinazoline-2-¹⁴C]TZB-30878 were determined using radio high-performance liquid chromatography on samples obtained after incubation with human hepatic microsomes. Eight metabolites were detected in the microsomal incubation mixture, and their structures were proposed by mass spectrometry techniques using TZB-30878 and two stable labeled TZB-30878 analogs, [quinoline-deuterium (D)₆]TZB-30878 and [piperazin-D₈]TZB-30878. Liquid chromatography/tandem mass spectrometry analyses suggested that the eight me-

tabolites consisted of a cyclic metabolite (M6), four hydroxylated metabolites (M1, M2, M3, and M4) (three on quinoline ring and one on quinazoline ring), a deaminated metabolite (M5), and two metabolites (M7 and M8) that were presumably intermediates leading to the formation of the cyclic metabolite M6. Hydroxylation sites in the quinoline and quinazoline rings were predicted by electron density calculations and confirmed by comparison with authentic standards. To the best of our knowledge, *N*-deamination by microsomes leading to the formation of M5 appears to be novel. In addition, *in vitro* experiments in human liver microsomes with cytochrome P450 (P450)-specific inhibitors revealed that CYP3A4 was the major enzyme responsible for the metabolism of TZB-30878. Other P450 enzymes, such as a CYP2D6, played a minor role in its metabolism.

Irritable bowel syndrome (IBS) is a common multifactorial disorder with a largely undefined etiology. Symptoms of IBS, such as abdominal pain and diarrhea, commonly develop and persist in patients who are in remission from other stress-related diseases. To develop a medication for patients with IBS, we focused on the properties of 5-hydroxytryptamine (5-HT)_{1A} agonism and 5-HT₃ antagonism and synthesized a novel compound, TZB-30878 (Fig. 1). This compound was expected to have anxiolytic action via 5-HT_{1A} agonism and to suppress intestinal motility and visceral hypersensitivity via 5-HT₃ antagonism. TZB-30878 was previously shown to exhibit potent and highly selective serotonin 5-HT₃ receptor antagonistic activities and also a high affinity for the 5-HT_{1A} receptor subtype that contributes to an overall therapeutic effect (Tamaoki et al., 2007). The pharmaco-

kinetics and excretion of TZB-30878 have been studied *in vivo* in rats previously (unpublished data). The results indicated that TZB-30878 is rapidly absorbed following *p.o.* administration, distributed to almost all the organs including brain, and eliminated into feces via bile. However, there is very limited information regarding metabolism of TZB-30878.

The objective of this study was to clarify the biotransformation of TZB-30878 in humans. We characterized the chemical structures of metabolites and identified the human hepatic cytochromes P450 (P450) responsible for the metabolism of TZB-30878.

Materials and Methods

Chemicals. Trifluoroacetic acid, Tris, potassium dihydrogen phosphate, dipotassium hydrogen phosphate, and ammonium acetate were purchased from Nacalai Tesque Inc. (Kyoto, Japan). α -Naphthoflavone, sulfaphenazole, quinidine hydrochloride, and diethylthiocarbamic acid sodium salt (diethylthiocarbamate) were purchased from Sigma-Aldrich (St. Louis, MO). β -NADP⁺,

Article, publication date, and citation information can be found at <http://dmd.aspetjournals.org>.

doi:10.1124/dmd.107.018168.

ABBREVIATIONS: IBS, irritable bowel syndrome; 5-HT, 5-hydroxytryptamine; TZB-30878, 3-amino-5,6,7,8-tetrahydro-2-[4-[4-(quinolin-2-yl)piperazin-1-yl]butyl]quinazolin-4(3H)-one; P450, cytochrome P450; G-6-P, *D*-glucose 6-phosphate disodium salt; D, deuterium; HPLC, high-performance liquid chromatography; LC, liquid chromatography; MS/MS, tandem mass spectrometry; M1, 3-amino-5,6,7,8-tetrahydro-2-[4-[4-(6-hydroxy-quinolin-2-yl)piperazin-1-yl]butyl]quinazolin-4(3H)-one; M2, 3-amino-5,6,7,8-tetrahydro-2-[4-[4-(7-hydroxy-quinolin-2-yl)piperazin-1-yl]butyl]quinazolin-4(3H)-one; M3, 3-amino-5,6,7,8-tetrahydro-2-[4-[4-(3-hydroxy-quinolin-2-yl)piperazin-1-yl]butyl]quinazolin-4(3H)-one; M4, 3-amino-6-hydroxy-5,6,7,8-tetrahydro-2-[4-[4-(quinolin-2-yl)piperazin-1-yl]butyl]quinazolin-4(3H)-one; M5, 5,6,7,8-tetrahydro-2-[4-[4-(quinolin-2-yl)piperazin-1-yl]butyl]quinazolin-4(3H)-one; M6, 2-hydroxy-2,3,4,5,7,8,9,10-octahydro[1,2]diazepino[7,1-b]quinazolin-11(1H)-one.

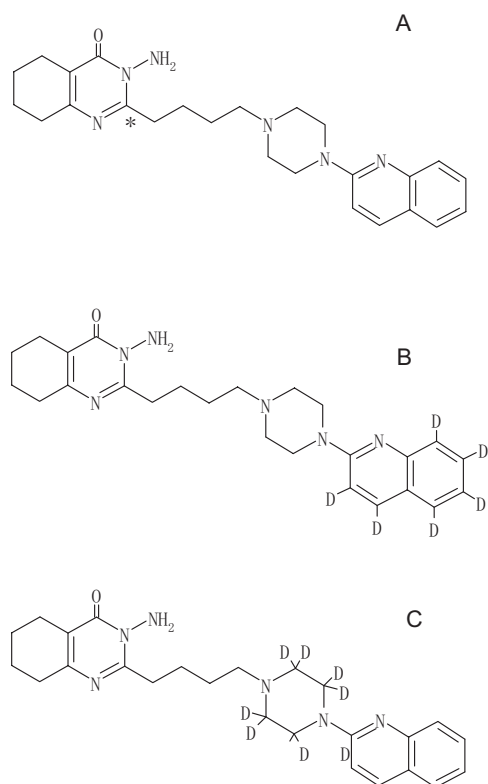


FIG. 1. Chemical structures of TZB-30878; *, denotes site of ^{14}C label (A), $[\text{D}_6]$ TZB-30878 (B), and $[\text{D}_8]$ TZB-30878 (C).

d-glucose 6-phosphate disodium salt (G-6-P), and glucose-6-phosphate dehydrogenase from yeast were purchased from the Oriental Yeast Co., Ltd. (Tokyo, Japan). HCl, acetonitrile, and methanol were purchased from Kanto Chemical Co. (Tokyo, Japan). Magnesium chloride hexahydrate, ketoconazole, and *S*-(+)-mephenytoin were purchased from Wako Pure Chemical Industries, Ltd. (Osaka, Japan), ICN Pharmaceuticals Inc. (Tokyo, Japan), and Ultra Fine Chemicals (Tokyo, Japan), respectively. TZB-30878, $[\text{deuterium} (\text{D})_6]$ TZB-30878, and $[\text{D}_8]$ TZB-30878 (Fig. 1) were prepared at the Synthetic Research Department of ASKA Pharmaceutical Co., Ltd. (Tokyo, Japan). TZB-30878 labeled with ^{14}C ($[\text{C}^{14}]$ TZB-30878) with a specific activity of 2.11 GBq/mmol and radiochemical purity >96.8% (Fig. 1) was prepared at GE Healthcare (Piscataway, NJ). Pooled, mixed gender, human hepatic microsomes and microsomes expressing human P450s from baculovirus-infected insect cells (human CYP1A1 + reductase microsomes, human CYP1A2 + reductase microsomes, human CYP1B1 + reductase microsomes, human CYP2A6 + reductase + b_5 microsomes, human CYP2B6 + reductase + b_5 microsomes, human CYP2C8 + reductase + b_5 microsomes, human CYP2C9*1 + reductase microsomes, human CYP2C9*2 + reductase microsomes, human CYP2C19 + reductase + b_5 microsomes, human CYP2D6*1 + reductase microsomes, human CYP2E1 + reductase + b_5 microsomes, human CYP3A4 + reductase + b_5 microsomes, human CYP4A11 + reductase microsomes, control microsomes, and control microsomes + reductase + b_5) were purchased from Gentest Corp. (Woburn, MA).

Analysis of $[\text{C}^{14}]$ TZB-30878 Metabolites. Analyses were performed on a high-performance liquid chromatography (HPLC) system (LC-10AD or LC-10AD_{VP}, Shimadzu Corp., Kyoto, Japan) equipped with a UV-visible detector (SPD-10A, SPD-10A_{VP}, or SPD-M10A_{VP}, Shimadzu) and radioactivity detector (RAD 525TR or 625TR, PerkinElmer Life and Analytical Sciences Inc., Boston, MA). The analytical column, a 5- μm , Inertsil Ph-3, 150 \times 4.6-mm column from GL Sciences (Tokyo, Japan), was maintained at 40°C. The mobile phase, consisting of 0.1% (v/v) trifluoroacetic acid (A) and acetonitrile (B), was maintained at a constant flow rate of 1.0 ml/min. UV detection of metabolites was performed at 249 nm. The elution gradient was 92.0% A, followed by a linear increase to 82.0% A in 40.00 min. At 40.01 min, the gradient was adjusted to achieve 70.0% A in 5 min. After liquid chromatog-

raphy (LC) analysis, the concentrations of the metabolites were calculated based on radiometric detection.

Structural Elucidation of TZB-30878 Metabolites. All the microsomal incubations contained 1 μM $[\text{D}_0/\text{D}_6]$ TZB-30878 (a mixture of equal parts TZB-30878 and $[\text{D}_6]$ TZB-30878) or 1 μM $[\text{D}_0/\text{D}_8]$ TZB-30878 (a mixture of equal parts TZB-30878 and $[\text{D}_8]$ TZB-30878), 0.5 mg protein/ml microsomes, and an NADPH-generating system consisting of 3.3 mM magnesium chloride, 1.3 mM NADP⁺, 3.3 mM G-6-P, 2.5 units/ml glucose-6-phosphate dehydrogenase from yeast, and 100 mM phosphate buffer in 1.0 ml, pH 7.4. Before the addition of the NADPH-generating system, the incubation mixtures were preincubated for 5 min at 37°C. The final concentration of the organic solvent in the incubation system was 1%. Reactions were initiated by the addition of the NADPH-generating system, then allowed to proceed for 20 min at 37°C, and terminated with 2 ml of ice-cold acetonitrile. The incubation mixtures were then sonicated for 5 min, centrifuged (1800g, 4°C, 5 min), and the supernatants obtained. The residue was mixed with an additional 2 ml of acetonitrile, and the extraction procedure was repeated. The supernatants from both extractions were combined and diluted to 5 ml with acetonitrile. The chemical structures of TZB-30878 metabolites were elucidated and identified with LC/tandem mass spectrometry (MS/MS). The LC/MS/MS system consisted of a Waters 2795 pump (Waters Corp., Milford, MA) and an MS/MS detector (Quattro Ultima Pt, Micromass Co., Manchester, UK) using electrospray ionization in the positive ion mode. The LC conditions were the same as those used for HPLC for the analysis of $[\text{C}^{14}]$ TZB-30878 metabolites. The chemical structures of the metabolites were identified by comparing the retention times and mass spectra on LC/MS/MS with those of authentic standards. Electron density was calculated by the AM1 method (Dewar et al., 1985) using MOPAC version 6.

Screening of Microsomes Expressing 13 Isoforms of Human P450s. In vitro screening of $[\text{C}^{14}]$ TZB-30878 with 13 microsomes expressing human P450s (CYP1A1, CYP1A2, CYP1B1, CYP2A6, CYP2B6, CYP2C8, CYP2C9*1, CYP2C9*2, CYP2C19, CYP2D6*1, CYP2E1, CYP3A4, and CYP4A11) was performed using a constant amount of P450 (20 pmol P450/0.5 mg protein/ml) and 1 μM $[\text{C}^{14}]$ TZB-30878. All the 20-min incubations with microsomes expressing human P450 were carried out, terminated, and analyzed as described above. Insect microsomes without human P450 cDNA were used as controls. For CYP2A6, CYP2C9*1, CYP2C9*2, and their controls, incubations were performed in 100 mM Tris-HCl buffer, pH 7.5.

Inhibition with Chemical Inhibitors. Inhibition of TZB-30878 metabolism was evaluated using chemical inhibitors. Human hepatic microsomes (0.5 mg protein/ml) or microsomes expressing human P450 (20 pmol P450/0.5 mg protein/ml) and 1 μM $[\text{C}^{14}]$ TZB-30878 were preincubated with various concentrations of inhibitors (α -naphthoflavone at 0.1, 1, and 10 μM ; sulfaphenazole at 0.3, 3, and 30 μM ; *S*-(+)-mephenytoin at 40, 400, and 4000 μM ; quinidine at 0.4, 4, and 40 μM ; diethyldithiocarbamate at 10, 100, and 1000 μM ; ketoconazole at 0.1, 1, and 10 μM) (Newton et al., 1995; Kilicarslan et al., 2001). The incubation and extraction conditions were the same as those described above. Sample mixed with methanol instead of inhibitor was used as a control.

Chemical Synthesis and Characterization of Authentic Standards. M1 through M6 were synthesized chemically (Fig. 2). Namely, alkylation of corresponding compound 4 with compound 2 (X = Y = H) in the presence of triethylamine gave the key compound 5. Cyclization of 5 with hydrazine gave M1, M2, and M3. Compound 6, synthesized using the same procedure (X = Y = ethylene ketal), was treated with acid and then reduced to give M4. M5 was synthesized by deamination of TZB-30878. Condensation of corresponding amine 1 with glutaric anhydride gave compound 7. Protection of the aldehyde group in 7 with ethylene glycol and cyclization with hydrazine gave compound 8. Deprotection with acid treatment gave M6. Structure characterization was accomplished using mass spectral analysis and standard NMR proton experiments. Mass spectra were collected using a Shimadzu QP-5000 system by the electron ionization method. NMR experiments were performed at 400 MHz on a JNM ECP-400 spectrometer (JEOL Ltd., Tokyo, Japan). Complete ^1H chemical shifts were obtained and reported in parts per million (Table 1).

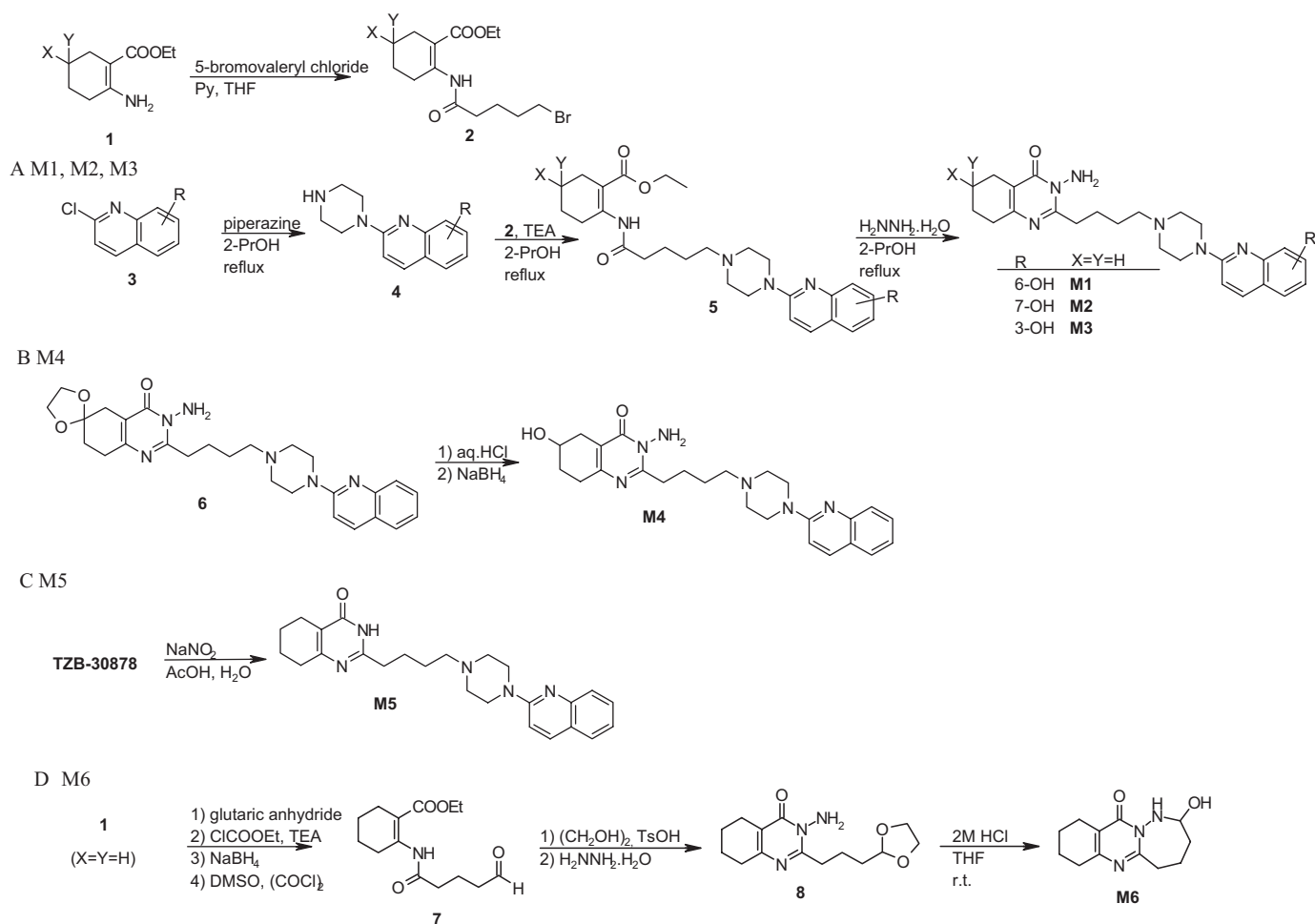


FIG. 2. Chemical synthetic routes for authentic metabolite samples.

TABLE 1

¹H NMR and mass spectral data of TZB-30878 and M1 through M6

Compound	Solvent	¹ H NMR (400 MHz) δ (ppm)	EI-MS
			<i>m/z</i>
TZB-30878	CDCl ₃	7.87 (d, <i>J</i> = 9.3 Hz, 1H), 7.69 (d, <i>J</i> = 8.5 Hz, 1H), 7.58 (d, <i>J</i> = 7.7 Hz, 1H), 7.52 (ddd, <i>J</i> = 1.5 Hz, 6.9 Hz, 7.5 Hz, 1H), 7.25–7.19 (m, 1H), 6.97 (d, <i>J</i> = 8.9 Hz, 1H), 4.93 (s, 2H), 3.74 (t, <i>J</i> = 5.0 Hz, 4H), 2.92 (t, <i>J</i> = 7.7 Hz, 2H), 2.58–2.55 (m, 6H), 2.52–2.49 (m, 2H), 2.44 (t, <i>J</i> = 7.3 Hz, 2H), 1.81–1.63 (m, 8H)	432 (M ⁺), 157 (base)
M1	Dimethyl sulfoxide-D ₆	9.36 (br s, 1H), 7.87 (d, <i>J</i> = 9.2 Hz, 1H), 7.44 (d, <i>J</i> = 8.9 Hz, 1H), 7.15 (d, <i>J</i> = 9.2 Hz, 1H), 7.09 (dd, <i>J</i> = 9.2 Hz, <i>J</i> = 2.7 Hz, 1H), 6.96 (d, <i>J</i> = 2.7 Hz, 1H), 5.75 (s, 2H), 3.30 (br s, 4H), 2.85–2.81 (m, 2H), 2.60–2.30 (m, 10H), 1.76–1.54 (m, 8H)	289, 173 (base), 144
M2	Dimethyl sulfoxide-D ₆	9.69 (br s, 1H), 7.86 (d, <i>J</i> = 9.2 Hz, 1H), 7.50 (d, <i>J</i> = 8.9 Hz, 1H), 6.95 (d, <i>J</i> = 9.2 Hz, 1H), 6.83 (d, <i>J</i> = 1.9 Hz, 1H), 6.76 (dd, <i>J</i> = 8.5 Hz, 2.3 Hz, 1H), 5.75 (s, 2H), 3.62 (br s, 4H), 2.85–2.81 (m, 2H), 2.60–2.30 (m, 10H), 1.76–1.52 (m, 8H)	432, 173 (base)
M3	CDCl ₃	7.86 (d, <i>J</i> = 8.9 Hz, 1H), 7.62 (d, <i>J</i> = 8.1 Hz, 1H), 7.47 (t, <i>J</i> = 6.9 Hz, 1H), 7.42 (s, 1H), 7.38–7.35 (m, 1H), 4.96 (s, 2H), 3.30 (m, 4H), 2.95–2.91 (m, 2H), 2.67 (br s, 4H), 2.59 (t, <i>J</i> = 6.2 Hz, 2H), 2.54–2.47 (m, 4H), 1.85–1.64 (m, 8H)	448 (M ⁺), 432, 289, 173 (base)
M4	CDCl ₃	7.88 (d, <i>J</i> = 9.2 Hz, 1H), 7.70 (d, <i>J</i> = 8.5 Hz, 1H), 7.70 (d, <i>J</i> = 8.5 Hz, 1H), 7.53 (ddd, <i>J</i> = 1.5 Hz, 6.9 Hz, 8.5 Hz, 1H), 7.22 (ddd, <i>J</i> = 1.2 Hz, 6.9 Hz, 8.1 Hz, 1H), 6.97 (d, <i>J</i> = 9.2 Hz, 1H), 4.97 (s, 2H), 4.24–4.16 (m, 1H), 3.75 (t, <i>J</i> = 5.0 Hz, 4H), 2.93 (t, <i>J</i> = 7.7 Hz, 2H), 2.88–2.76 (m, 2H), 2.69–2.49 (m, 6H), 2.45 (t, <i>J</i> = 7.3 Hz, 2H), 2.01–1.61 (m, 6H)	448 (M ⁺), 157 (base)
M5	CDCl ₃	12.27 (br s, 1H), 7.87 (d, <i>J</i> = 9.2 Hz, 1H), 7.68 (d, <i>J</i> = 8.5 Hz, 1H), 7.59–7.57 (m, 1H), 7.21 (ddd, <i>J</i> = 8.1 Hz, <i>J</i> = 6.9 Hz, <i>J</i> = 1.2 Hz, 1H), 6.96 (d, <i>J</i> = 9.2 Hz, 1H), 3.80–3.78 (m, 4H), 2.69–2.65 (m, 2H), 2.62–2.57 (m, 6H), 2.50–2.43 (m, 4H), 1.86–1.60 (m, 8H)	417 (M ⁺), 204, 157 (base)
M6	CDCl ₃	7.03–6.99 (m, 1H), 4.96 (br s, 1H), 3.15–3.08 (m, 1H), 2.91–2.86 (m, 1H), 2.61–2.59 (m, 2H), 2.52–2.50 (m, 2H), 1.94–1.92 (m, 2H), 1.83–1.70 (m, 6H)	235 (M ⁺), 217, 179 (base)

Results

When [^{14}C]TZB-30878 (Fig. 1) was incubated with pooled, mixed gender, human hepatic microsomes and an NADPH-generating system, eight metabolites (M1–8) were found by radiometric detection (Fig. 3). The metabolites (M1–8) accounted for approximately 12.6, <5.0, 6.7, <5.0, 12.2, 10.8, 6.7, and 5.2% of the injected radioactivity, respectively. The structures of the metabolites were proposed by LC/MS/MS in tandem with electron density calculations and confirmed by direct comparison with authentic standards. In addition, human P450 enzymes involved in the metabolisms of TZB-30878 were identified by screening of microsomes expressing 13 isoforms of human P450s and through an inhibition study.

Identification of Metabolites. Structural elucidation was con-

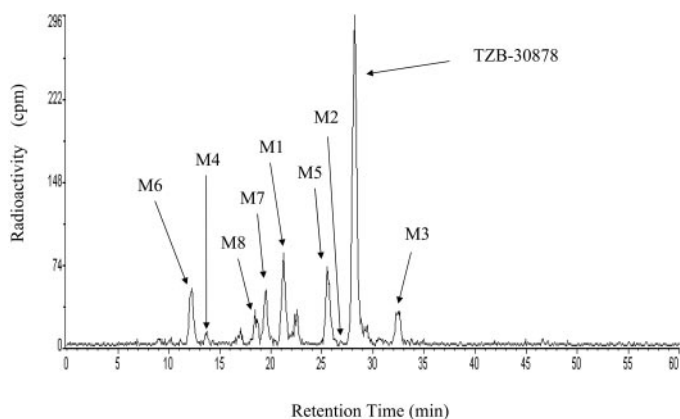


FIG. 3. Representative HPLC radioactivity profile of TZB-30878 metabolites in a human hepatic microsome incubation. Incubations were carried out at 37°C for 20 min using human hepatic microsomes and [^{14}C]TZB-30878 (1 μM) with NADPH-generating system.

ducted with the aid of two stable isotope-labeled TZB-30878 compounds ($[\text{D}_6]$ TZB-30878 and $[\text{D}_8]$ TZB-30878) that served to detect metabolites and facilitate structural identification. To elucidate the chemical structures of TZB-30878 metabolites, the fragmentation pattern of TZB-30878 was first examined. This showed the formation of major fragment ions (220 and 171) via breaking of the piperazine ring (Fig. 4). The position of the stable label aided in the elucidation of structure by producing differentially labeled fragment ions on collisional activation. The elucidation of metabolite structure was performed by acquiring collision-induced dissociation mass spectra using a linked sector scan (i.e., MS/MS).

The MS/MS spectrum of M1 (Fig. 5) was similar to that of M2 and M3. The mass spectra of M1, M2, and M3 from TZB-30878 and $[\text{D}_8]$ TZB-30878 showed a protonated molecular ion at m/z 449 and 457, respectively. On the other hand, the mass spectra of M1, M2, and M3 from $[\text{D}_6]$ TZB-30878 showed a protonated molecular ion at m/z 454. Likewise, the mass spectra from TZB-30878, $[\text{D}_6]$ TZB-30878, and $[\text{D}_8]$ TZB-30878 showed a fragment ion at m/z 230, 235, and 238, respectively. These findings indicated that a hydroxy group was introduced to the quinoline ring. The electron densities of the parent compound are shown in Fig. 6. The results indicated that the positions of high electron density in the quinoline ring were C-3, C-6, and C-7, and M1, M2, and M3 were predicted to have the hydroxy metabolites at C-3, C-6, and C-7 in the quinoline ring. The structures of M1, M2, and M3 were confirmed by comparing the retention times and mass spectra with those of authentic standards by LC/MS/MS.

The MS/MS spectra of M4 from TZB-30878, $[\text{D}_6]$ TZB-30878, and $[\text{D}_8]$ TZB-30878 showed a protonated molecular ion at m/z 449, 455, and 457, respectively (Fig. 7), indicating the addition of a hydroxy group to the quinazoline ring or linker moiety. In addition, the mass spectra showed a fragment ion at m/z 236, indicating a hydroxy group that was introduced to the quinazoline ring. Because the positions of

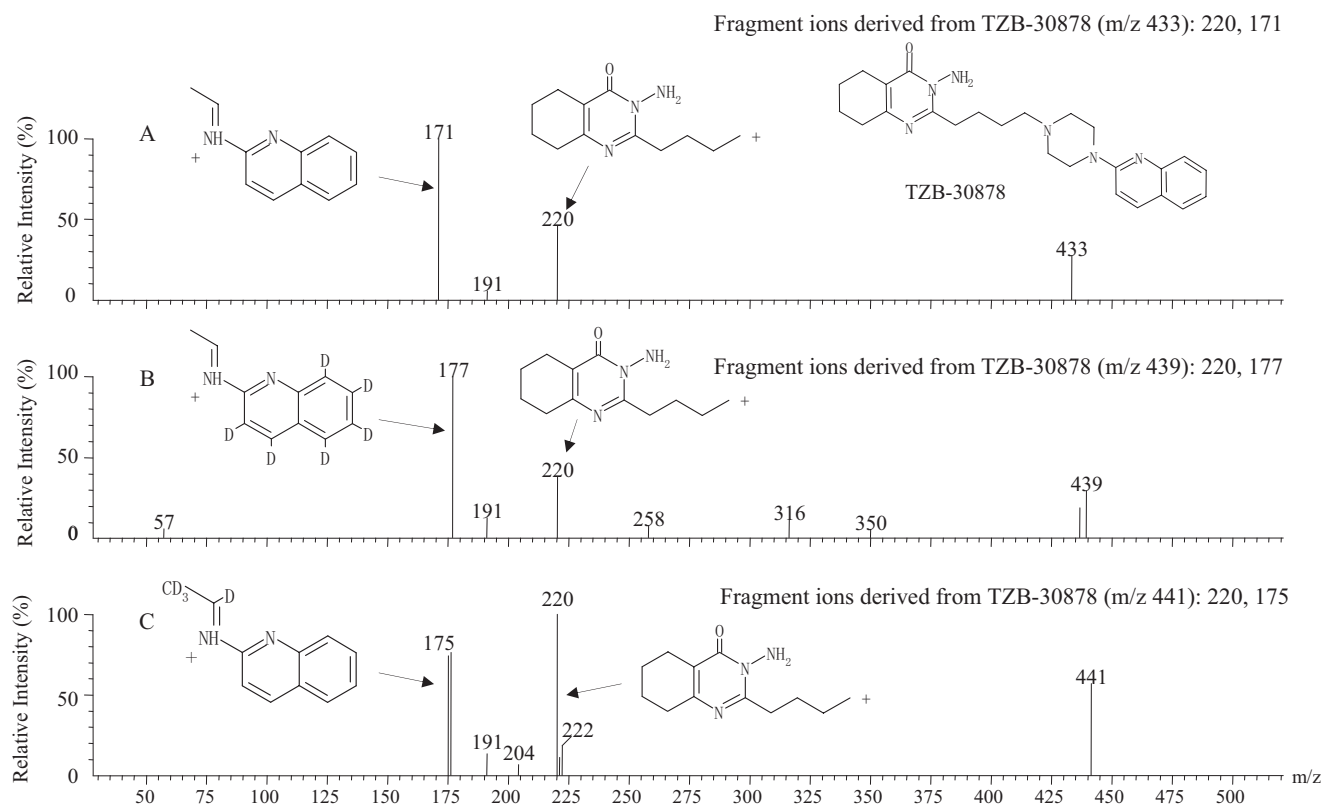


FIG. 4. Structure and MS/MS spectra of TZB-30878 (A), $[\text{D}_6]$ TZB-30878 (B), and $[\text{D}_8]$ TZB-30878 (C).

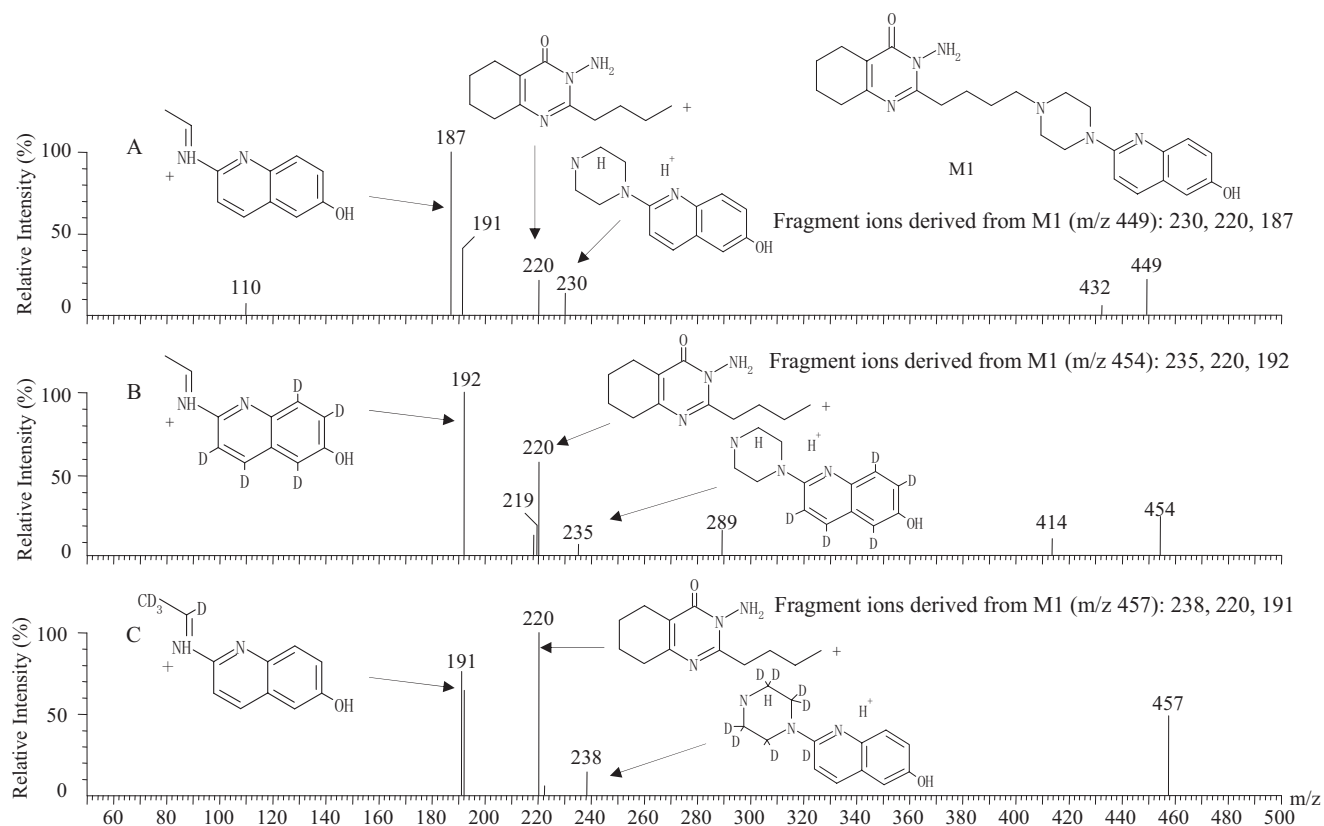


FIG. 5. Structure and MS/MS spectra of M1 from TZB-30878 (A), $[D_6]$ TZB-30878 (B), and $[D_8]$ TZB-30878 (C). Incubations were carried out at 37°C for 20 min using human hepatic microsomes and $[D_6/D_8]$ TZB-30878 (1 μ M) or $[D_6/D_8]$ TZB-30878 (1 μ M) with NADPH-generating system.

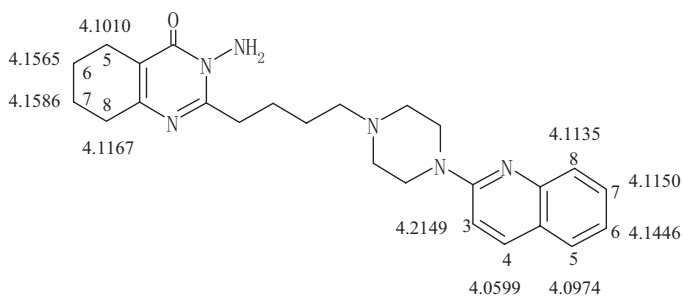


FIG. 6. Electron densities of TZB-30878 calculated by the AM1 method.

high electron density in the quinazoline ring were C-6 and C-7 (Fig. 6), it was predicted that M4 had a hydroxy metabolite at C-6 or C-7 in the quinazoline ring. The structure of M4 was confirmed by comparing the retention time and mass spectrum with those of the authentic standard by LC/MS/MS.

The MS/MS spectra of M5 from TZB-30878, $[D_6]$ TZB-30878, and $[D_8]$ TZB-30878 showed a protonated molecular ion at m/z 418, 424, and 426, respectively (Fig. 8), which was 15 atomic mass units less than those of the unchanged compounds. The mass spectra also showed a fragment ion at m/z 214, 220, and 222, respectively. Another fragment ion was shown at m/z 205 instead of 220, indicating the lack of an amino group. The structure of M5 was confirmed by comparing the retention time and mass spectrum with those of the authentic standard by LC/MS/MS.

The MS/MS spectra of M6 from TZB-30878, $[D_6]$ TZB-30878, and $[D_8]$ TZB-30878 showed a protonated molecular ion at m/z 236 (Fig. 9). This result indicated that M6 did not have a piperazine ring or quinoline ring. The fragment ion was shown at m/z 218, suggesting

that M6 had a hydroxy group that could be dehydrated. It is known that breaking of the C-N bond between an alkyl group and piperazine ring can occur (Zhu et al., 2005). Our findings suggested that M6 might be a cyclic form arising via cyclization of the aldehyde form (Thompson et al., 1996, 2000; Singh et al., 2003). The structure of M6 was confirmed by comparing the retention time and mass spectrum with those of the authentic standard by LC/MS/MS.

The mass spectra of M7 from TZB-30878, $[D_6]$ TZB-30878, and $[D_8]$ TZB-30878 showed a protonated molecular ion at m/z 449, 455, and 457, respectively, indicating the addition of a hydroxy group to the quinazoline ring or linker moiety. The MS/MS spectra also showed a fragment ion at m/z 431, 437, and 439, respectively (Fig. 10). Likewise, fragment ions were shown at m/z 214, 220, and 222, respectively. These findings suggested that the metabolite had a hydroxyl group that could be dehydrated. Namely, the hydroxy group might be introduced to the linker moiety. It could be predicted that breaking of the C-N bond between the linker moiety and piperazine ring was initiated through hydroxylation at the linker moiety. Our findings suggested that M7 was 3-amino-5,6,7,8-tetrahydro-2-(4-hydroxy-4-[4-(quinolin-2-yl)piperazin-1-yl]butyl)quinazolin-4(3H)-one (Fig. 10).

The MS/MS spectra of M8 from TZB-30878, $[D_6]$ TZB-30878, and $[D_8]$ TZB-30878 showed a protonated molecular ion at m/z 236. This result indicated that M8 did not have a piperazine ring or quinoline ring. The absence of a fragment ion at m/z 218 indicated that the metabolite did not have a hydroxy group that could be dehydrated. These findings suggested that M8 was an intermediate between M7 and M6. M8 was predicted to be 4-(3-amino-4-oxo-3,4,5,6,7,8-hexahydroquinazolin-2-yl)butanal (Fig. 11). The chemical structure of the metabolite with retention times of 17.0 and 22.4 min could not be determined (Fig. 3).

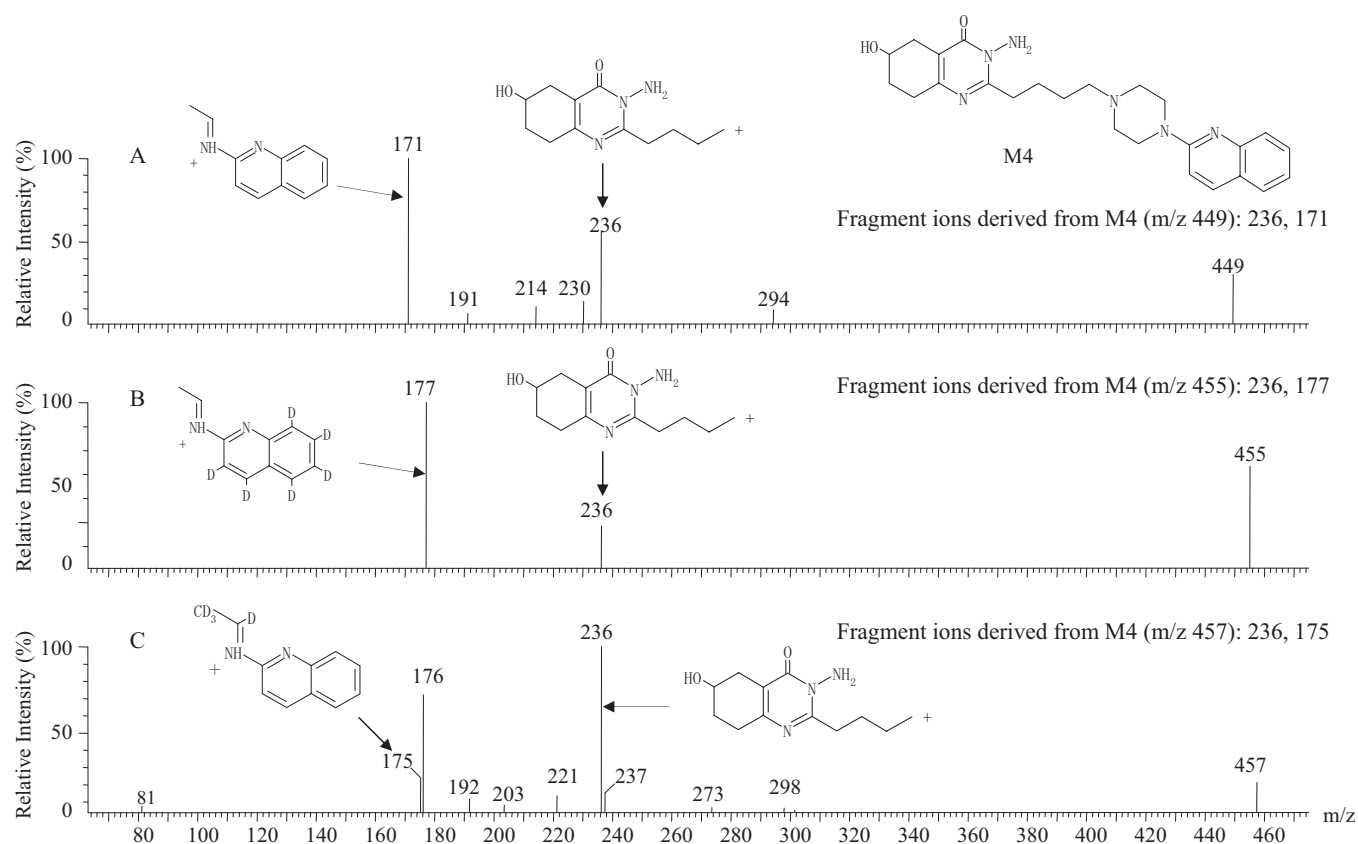


Fig. 7. Structure and MS/MS spectra of M4 from TZB-30878 (A), $[D_6]$ TZB-30878 (B), and $[D_8]$ TZB-30878 (C). Incubations were carried out at 37°C for 20 min using human hepatic microsomes and $[D_6/D_6]$ TZB-30878 (1 μ M) or $[D_8/D_8]$ TZB-30878 (1 μ M) with NADPH-generating system.

Screening of Microsomes Expressing Human P450. P450s involved in the metabolism of TZB-30878 were determined by using microsomes expressing human P450. $[^{14}C]$ TZB-30878 at a final concentration 1 μ M was incubated with P450-expressing microsomes at a final concentration of 20 pmol P450/0.5 mg protein/ml for 20 min, and the incubation mixture was analyzed by HPLC. The results indicated that TZB-30878 was metabolized by incubation with CYP1A1, CYP2D6*1, and CYP3A4 as shown in Fig. 12. The disappearance rate of TZB-30878 was fast and in the following order: CYP3A4 > CYP1A1 > CYP2D6*1. CYP1A1 was mainly involved in the formation of M1 and M6; CYP2D6*1 was mainly involved in the formation of M7; and CYP3A4 was mainly involved in the formation of M1, M3, M5, M6, and M7. The above results suggested that TZB-30878 was metabolized most markedly by CYP3A4, and that CYP1A1 and CYP2D6*1 were possibly involved in the metabolism.

Inhibition Study. P450s involved in the metabolism of TZB-30878 were examined using inhibitors against the P450s. $[^{14}C]$ TZB-30878 at a final concentration of 1 μ M was incubated with human hepatic microsomes at a final concentration 0.5 mg of protein/ml. Next, each typical inhibitor against P450 was added for 20 min, and the incubation mixture was analyzed by HPLC. The results were evaluated based on the percentage of control, which was defined as the percentage of the metabolic activity in the presence of inhibitor to that of metabolic activity in the absence of inhibitor (Table 2). The elimination of TZB-30878 was markedly inhibited by addition of 0.1, 1, and 10 μ M ketoconazole, resulting in 63.9, 99.8, and 100.0% of inhibition, respectively. *S*-(+)-Mephenytoin (4000 μ M), quinidine (40 μ M), and diethyldithiocarbamate (1000 μ M) slightly inhibited TZB-30878 metabolism, resulting in 51.9, 43.0, and 35.1% of inhibition, respec-

tively. The formation of metabolites was also clearly inhibited by ketoconazole. These results suggested that TZB-30878 was mainly metabolized by CYP3A4 and partially metabolized by CYP2D6.

Discussion

In the present study, formation of TZB-30878 metabolites was investigated using human hepatic microsomes. In addition, P450s involved in metabolism were determined by using microsomes expressing human P450s and inhibitors against human P450s. A proposed biotransformation pathway for TZB-30878 is provided in Fig. 13.

The chemical structures of the TZB-30878 metabolites were elucidated using $[D_6/D_6]$ TZB-30878 and $[D_6/D_8]$ TZB-30878, where $[D_6]$ TZB-30878 was a compound labeled with D at the quinoline ring of TZB-30878 and $[D_8]$ TZB-30878 was a compound labeled with D at the piperazine ring. Two mixtures of equal parts labeled and nonlabeled compound allowed rapid detection and structural elucidation of metabolites. By looking for molecular ion clusters of M/M+6 and M/M+8, the fragmentation behavior of TZB-30878 and its metabolites, as well as structural confirmation, was readily available. In addition, oxidative metabolites of TZB-30878 were separated by LC/MS/MS. LC/MS/MS analyses revealed that M1, M2, and M3 contained a hydroxyl group (+O) in the quinoline ring and M4 and M7 contained a hydroxy group (+O) in the quinazoline ring or linker moiety. It was also determined that M5 lost the amino group of the quinazoline ring. *N*-Deamination represents a novel biotransformation pathway.

Electronic characteristics play a role in the position of substrate oxidation of P450s. For example, the tendency toward oxidation of a certain functional group generally follows the relative stability of the

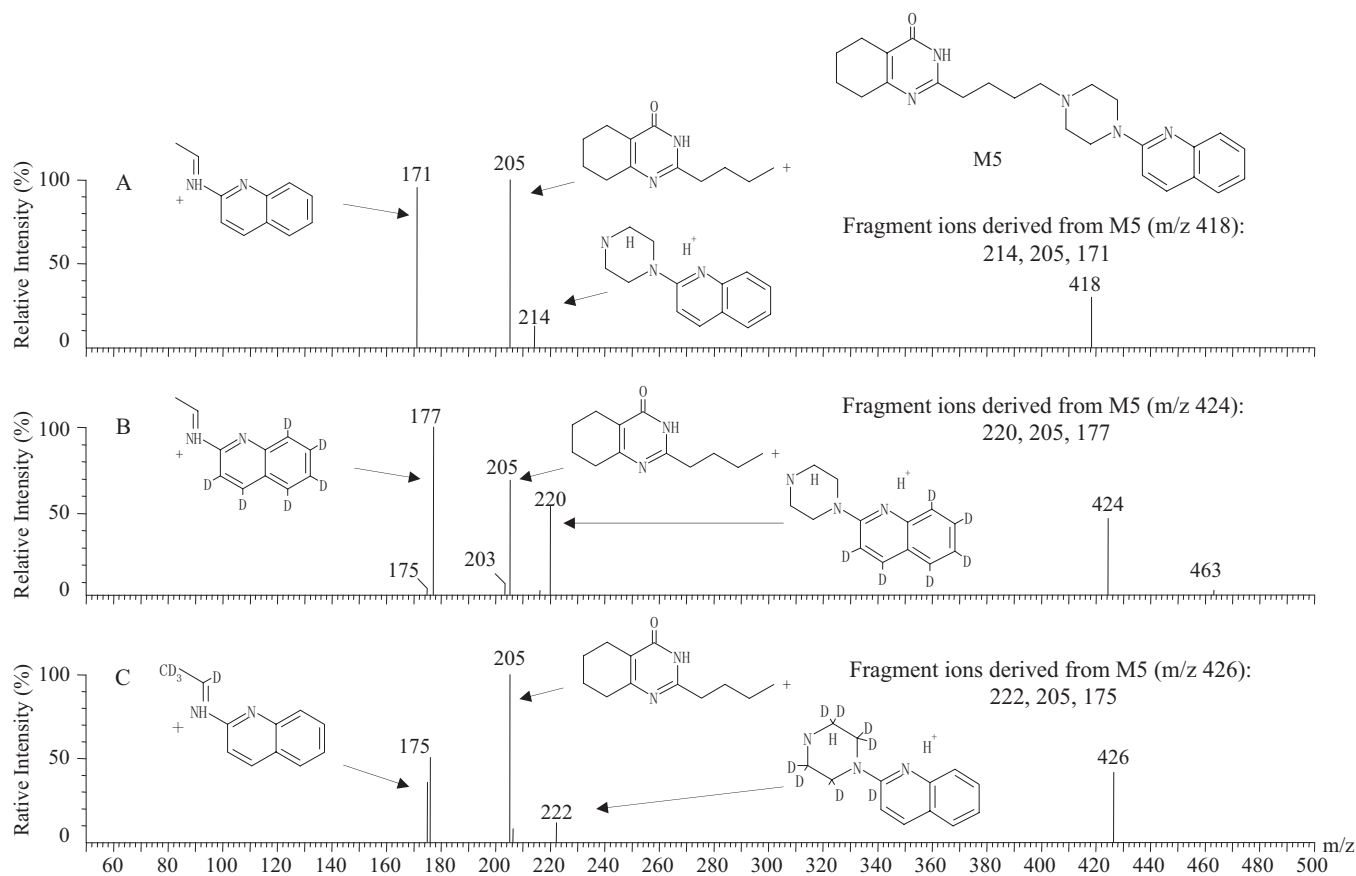


FIG. 8. Structure and MS/MS spectra of M5 from TZB-30878 (A), $[D_6]$ TZB-30878 (B), and $[D_8]$ TZB-30878 (C). Incubations were carried out at 37°C for 20 min using human hepatic microsomes and $[D_0/D_6]$ TZB-30878 (1 μ M) or $[D_0/D_8]$ TZB-30878 (1 μ M) with NADPH-generating system.

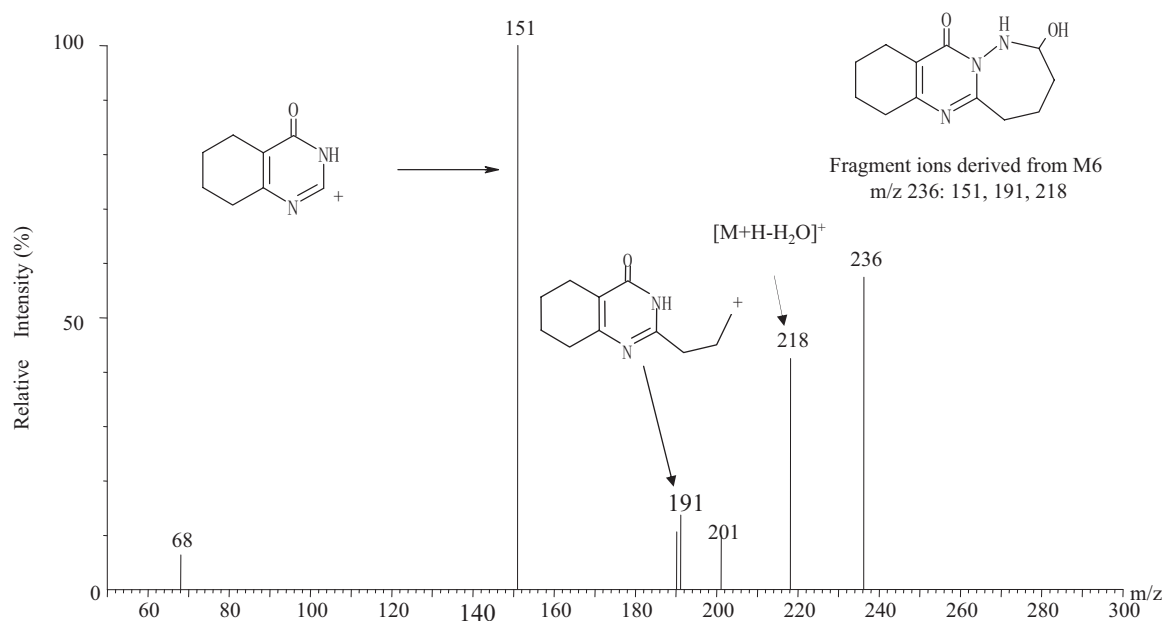


FIG. 9. Structure and MS/MS spectrum of M6 from TZB-30878. Incubations were carried out at 37°C for 20 min using human hepatic microsomes and $[D_0/D_8]$ TZB-30878 (1 μ M) with NADPH-generating system.

radicals that are formed, e.g., *N*-dealkylation > *O*-dealkylation > 2° carbon oxidation > 1° carbon oxidation. The chemical structures of M1, M2, and M3 were predicted by calculated electronic characteristics and then identified by comparing the characteristics with the

authentic standards. The chemical structure of M4 was also predicted by calculated electronic characteristics and identified by comparing with the authentic standard. Our results showed a useful correlation between the oxidation sites and electronic characteristics.

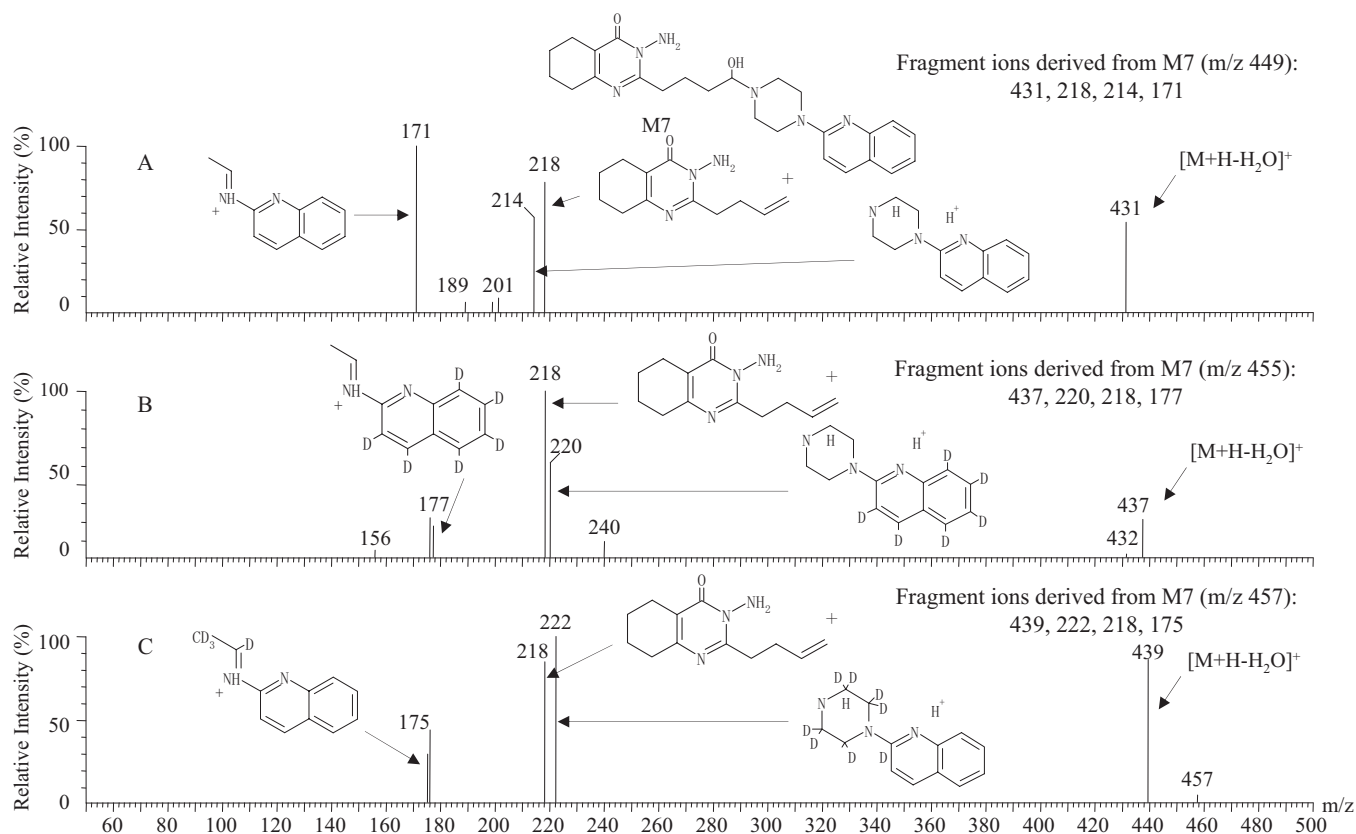


FIG. 10. Structure and MS/MS spectra of M7 from TZB-30878 (A), $[D_6]$ TZB-30878 (B), and $[D_8]$ TZB-30878 (C). Incubations were carried out at 37°C for 20 min using human hepatic microsomes and $[D_6/D_8]$ TZB-30878 (1 μ M) or $[D_6/D_8]$ TZB-30878 (1 μ M) with NADPH-generating system.

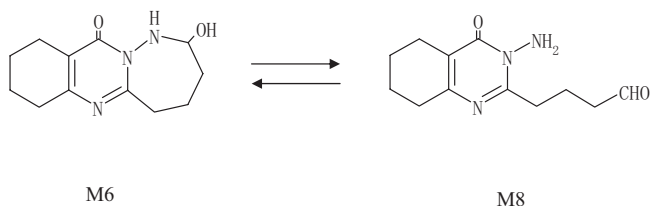


FIG. 11. Proposed reversible conversion of M8 into M6.

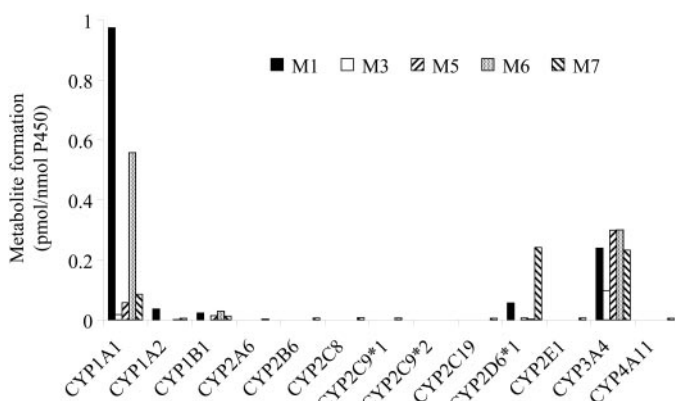


FIG. 12. Screening of TZB-30878 with 13 microsomes expressing human P450 for the formation of metabolites.

We confirmed the formation of the cyclic metabolite M6. At the time of M6 formation, quipazine, a nonselective 5-HT agonist, was released. The pharmacological activity was much lower than that of TZB-30878 (Brumley and Robinson, 2005). One of the major meta-

bolic pathways was caused by formation of the cyclic metabolite M6 via intermediates M7 and M8. In some cases the products can rearrange to form new heterocyclic rings (O'Donnell et al., 1979; Nikolic et al., 2004). Acetaldehyde and hydrazine react to form a hydrazone (Schiff base), which cyclizes on oxidation to methyltriazolophthalazine. The kinetics of the reaction to form methyltriazolophthalazine has been studied at 37°C and other temperatures at physiological pH and concentrations (O'Donnell et al., 1979). In rats, lidocaine metabolite reacts with the aldehyde to form a heterocyclic compound (Nelson et al., 1973), and acetaldehyde reacts with dopamine, resulting in pharmacologically active compounds (Collins et al., 1979). In this study, the aldehyde form M8 was also proposed as an intermediate to M6, but the aldehyde form could have undergone a reversible cyclization to M6.

P450 reaction phenotyping of TZB-30878 was performed using a combination of two basic approaches (Bjornsson et al., 2003). The first approach was to determine whether heterologously expressed, recombinant human P450s were capable of metabolizing TZB-30878. The second approach was to examine the metabolic reaction in the absence and presence of P450-specific chemical inhibitors. Using microsomes expressing human P450, CYP1A1, CYP1B1, CYP2D6*1, and CYP3A4 were found to be involved in TZB-30878 metabolism. Using typical inhibitors with human hepatic microsomes, CYP2C19, CYP2D6, CYP2E1, and CYP3A4 were found to be involved in TZB-30878 metabolism. Formation of M1, M3, M5, M6, and M7 was mediated via CYP3A4 based on the formation of the metabolites from microsomes expressing human CYP3A4. Ketoconazole is a known selective inhibitor of CYP3A4 (Wrighton and Ring, 1994; Ghosal et al., 1996; Desai et al., 1998; Masimirembwa et al., 1999), and production of M1, M3, M5, M6, and M7 by human hepatic

TABLE 2

Effect of P450 inhibitors on the metabolism of TZB-30878 with human hepatic microsomes

Percent of inhibition = $(A - B)/A \times 100$ (A, metabolic activity in the absence of inhibitor; B, metabolic activity in the presence of inhibitor).

Inhibitor	μM	% of Inhibition					
		TZB-30878	M1	M3	M5	M6	M7
α -Naphthoflavone CYP1A	0.1	8.6	-3.2	16.4	1.6	17.6	7.7
	1	0.8	0.0	-3	0.0	23.1	11.5
	10	7.2	0.0	10.4	-4.9	25.0	9.6
Sulfaphenazole CYP2C9	0.3	9.8	5.6	11.9	-5.7	28.7	19.2
	3	8.9	10.3	13.4	3.3	19.4	0.0
	30	16.7	13.5	32.8	9.0	33.3	42.3
S-(+)-Mephenytoin CYP2C19	40	9.8	4.8	14.9	1.6	32.4	34.6
	400	15.9	-11.1	47.8	21.3	50.0	36.5
	4000	51.9	26.2	89.6	85.2	78.7	100.0
Quinidine CYP2D6	0.4	10.9	3.2	4.5	2.5	25.9	0.0
	4	17.9	8.7	25.4	3.3	23.1	23.1
	40	43.0	21.4	43.3	25.4	56.5	100.0
Ketoconazole CYP3A4	0.1	63.9	53.2	62.7	47.5	75.9	100.0
	1	99.8	91.3	100.0	100.0	100.0	100.0
	10	100.0	100.0	100.0	100.0	100.0	100.0
Diethyldithiocarbamate CYP2E1	10	9.3	4.7	25.8	-9	17.9	10.4
	100	5.9	10.9	16.1	-18	16.8	-2.1
	1000	35.1	36.7	43.5	16.2	41.1	62.5

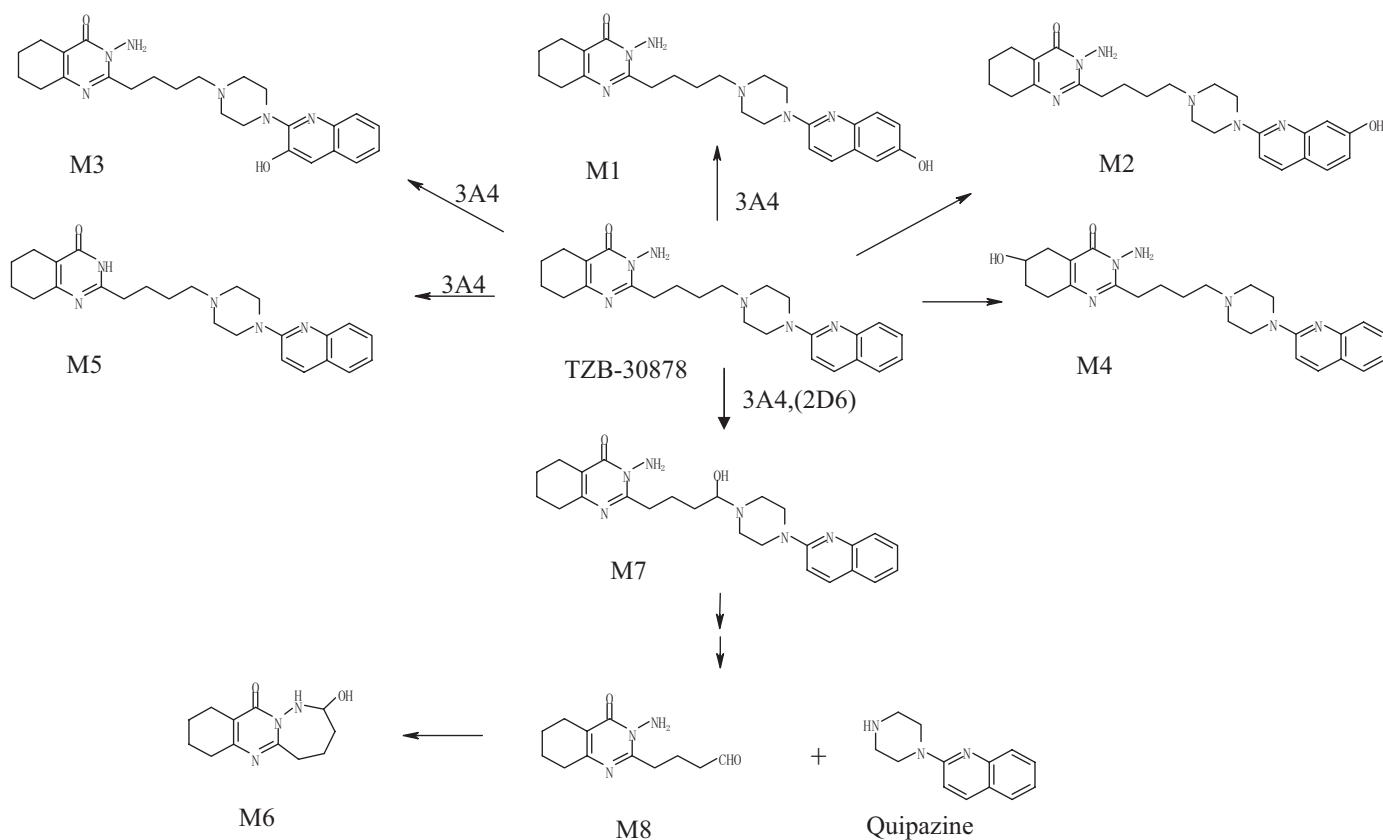


FIG. 13. Proposed biotransformation pathways of TZB-30878 in human hepatic microsomes. The primary P450 enzyme responsible for major biotransformation pathways in human hepatic microsomes is also listed.

microsomes was inhibited by ketoconazole. The formation of M1 and M7 with CYP2D9 suggested minor involvement of these enzymes in the metabolism of TZB-30878. We also observed that the CYP1A1/2-specific inhibitor α -naphthoflavone (Ghosal et al., 1996; Masimirembwa et al., 1999) caused no substantial inhibition of the metabolites M1 and M6. It was concluded that the contribution of CYP1A1 and CYP1B1 was negligible because of the very low ex-

pression level in human liver and intestine (Paine et al., 2006). However, there was slight stimulation of M5 and M7 formation with 10 μM α -naphthoflavone. Activation of CYP3A activity by α -naphthoflavone has been previously reported (Guengerich et al., 1994; Ghosal et al., 1996; Koley et al., 1997; Ueng et al., 1997). These results clearly indicated that CYP3A4 is the main contributor to TZB-30878 metabolism in human liver. N-Deamination by CYP3A4

represents a novel biotransformation pathway. In addition, CYP2D6 also slightly contributed to the TZB-30878 metabolism, but the contribution of CYP1A1 was negligible because of the low expression level in human liver.

The contribution of CYP2C19 and CYP2E1 should be discussed. The highest concentration of *S*-(+)-mephenytoin and diethyldithiocarbamate moderately inhibited TZB-30878 metabolism. However, insufficiency of the selectivity to each P450 should be taken into consideration for the inhibition condition. This overestimation was consistent with the fact that TZB-30878 was not metabolized by CYP2C19- and CYP2E1-expressing microsomes. Identification of the CYP3A4 responsible for TZB-30878 metabolism will prove to be an invaluable tool in identifying the magnitude of drug-drug interactions.

In summary, the results of this study provide the first analysis of the biotransformation of TZB-30878 in humans. Metabolites were produced with human hepatic microsomes and the chemical structures identified by the ion cluster method using two kinds of labeled compounds mixtures and also by electronic characteristics. One of the major metabolic pathways was caused by the formation of the cyclic metabolite M6 via the intermediate M7. The formation of metabolites was mediated via CYP3A4, and CYP2D6 was slightly involved in the metabolism.

References

- Bjornsson TD, Callaghan JT, Einolf HJ, Fischer V, Gan L, Grimm S, Kao J, King SP, Miwa G, Ni L, et al. (2003) The conduct of in vitro and in vivo drug-drug interaction studies: a Pharmaceutical Research and Manufacturers of America (PhRMA) perspective. *Drug Metab Dispos* **31**:815–832.
- Brumley MR and Robinson SR (2005) The serotonergic agonists quipazine, CGS-12066A, and α -methylserotonin alter motor activity and induce hindlimb stepping in the intact and spinal rat fetus. *Behav Neurosci* **119**:821–833.
- Collins MA, Nijm WP, Borge GF, Teas G, and Goldfarb C (1979) Dopamine-related tetrahydroisoquinolines: significant urinary excretion by alcoholics after alcohol consumption. *Science* **206**:1184–1186.
- Desai PB, Duan JZ, Zhu YW, and Kouzi S (1998) Human liver microsomal metabolism of paclitaxel and drug interaction. *Eur J Drug Metab Pharmacokinet* **23**:417–424.
- Dewar MJS, Zoebisch EG, Healy EF, and Stewart JJP (1985) AM1: a new general purpose quantum mechanical molecular model. *J Am Chem Soc* **107**:3902–3909.
- Ghosal A, Satoh H, Thomas PE, Bush E, and Moore D (1996) Inhibition and kinetics of cytochrome P450 3A activity in microsomes from rat, human and cDNA-expressed human cytochrome P450. *Drug Metab Dispos* **24**:940–947.
- Guengerich FP, Kim B-R, Gillam EMJ, and Shimada T (1994) Mechanisms of enhancement and inhibition of cytochrome P450 catalytic activities, in *Proceedings of the 8th International Conference on Cytochrome P450 Biochemistry, Biophysics, and Molecular Biology* (Lechner MC ed) pp 97–101, John Libbey Eurotext, Paris.
- Kilicarslan T, Haining RL, Rettie AE, Busto U, Tyndale RF, and Sellers EM (2001) Flunitrazepam metabolism by cytochrome P450s 2C19 and 3A4. *Drug Metab Dispos* **29**:460–465.
- Koley AP, Buters JT, Robinson RC, Markowitz A, and Friedman FK (1997) Differential mechanisms of cytochrome P450 inhibition and activation by α -naphthoflavone. *J Biol Chem* **272**:3149–3152.
- Masimirembwa CM, Otter C, Berg M, Jonsson M, Leidvik B, Jonsson E, Johansson T, Backman A, Edulund A, and Andresson TB (1999) Heterologous expression and kinetic characterization of human cytochrome P-450: validation of a pharmacological tool for drug metabolism research. *Drug Metab Dispos* **27**:1117–1122.
- Nelson SD, Breck GD, and Trager WF (1973) In vivo metabolite condensations. Formation of N1-ethyl-2-methyl-N3-(2,6-dimethylphenyl)-4-imidazolidinone from the reaction of a metabolite of alcohol with a metabolite of lidocaine. *J Med Chem* **16**:1106–1112.
- Newton DJ, Wang RW, and Lu AY (1995) Cytochrome P450 inhibitors. Evaluation of specificities in the in vitro metabolism of therapeutic agents by human liver microsomes. *Drug Metab Dispos* **23**:154–158.
- Nikolic D, Li Y, Chadwick LR, Grubjesic S, Schwab P, Metz P, and van Breeman RB (2004) Metabolism of 8-prenylnargenin, a potent phytoestrogen from hops (*Humulus lupulus*), by human liver microsomes. *Drug Metab Dispos* **32**:272–279.
- O'Donnell JP, Proveaux WJ, and Ma JHK (1979) Kinetics studies of hydrazine reaction with acetaldehyde. *J Pharm Sci* **68**:1256–1258.
- Paine MP, Hart HL, Ludington SS, Haining RL, Rettie AE, and Zeldin DC (2006) The human intestinal cytochrome P450 "pie." *Drug Metab Dispos* **34**:880–886.
- Singh SB, Shen LQ, Walker MJ, and Sheridan RP (2003) A model for predicting likely sites of CYP3A4-mediated metabolism on drug-like molecules. *J Med Chem* **46**:1330–1336.
- Tamaoki S, Yamauchi Y, Nakano Y, Sakano S, Asagarsu A, and Sato M (2007) Pharmacological properties of 3-amino-5,6,7,8-tetrahydro-2-[4-[4-(quinolin-2-yl)piperazin-1-yl]butyl]quinazolin-4(3H)-one (TZB-30878), a novel therapeutic agent for diarrhea-predominant irritable bowel syndrome (IBS) and its effects on an experimental IBS model. *J Pharmacol Exp Ther* **322**:1–9.
- Thompson C, Kinter M, and Macdonald T (1996) Synthesis and in vitro reactivity of 3-carbamoyl-2-phenylpropionaldehyde and 2-phenylpropenal: putative reactive metabolites of felbamate. *Chem Res Toxicol* **9**:1225–1229.
- Thompson CD, Miller TA, Barthen MT, Dieckhaus CM, Sofia RD, and Macdonald TL (2000) The synthesis, in vitro reactivity, and evidence for formation in humans of 5-phenyl-1,3-oxazinane-2,4-dione, a metabolite of felbamate. *Drug Metab Dispos* **28**:434–439.
- Ueng Y-F, Kuwabara T, Chun Y-J, and Guengerich FP (1997) Cooperativity in oxidations catalyzed by cytochrome P450 3A4. *Biochemistry* **36**:370–381.
- Wrighton SA and Ring BJ (1994) Inhibition of human CYP3A catalyzed 1'-hydroxy midazolam formation by ketoconazole, nifedipine, erythromycin, cimetidine, and nizatidine. *Pharm Res* **11**:921–924.
- Zhu M, Zhao W, Jimenez H, Zhang D, Yeola S, Dai R, Vachharajani N, and Mitroka J (2005) Cytochrome P450 3A-mediated of buspirone in human liver microsomes. *Drug Metab Dispos* **33**:500–507.

Address correspondence to: Dr. Kouichi Minato, Pharmacokinetics Research Department, ASKA Pharmaceutical Co., Ltd., 1604 Shimosakunobe, Takatsu-ku, Kawasaki, 213-8522, Japan. E-mail: minato-k@aska-pharma.co.jp